

Characterization of *Citrus maxima* CYP86A22-like gene involved in stem and fruit development

Minmin Xi¹, Min Liu¹, Tao Ye¹, Xiaoqin Jin¹, Liangmiao Liu¹, Zhiting Deng¹ and Changchun Wang^{1*}

Crop Breeding and Applied Biotechnology
25(2): e48312521, 2025
Brazilian Society of Plant Breeding.
Printed in Brazil
<http://dx.doi.org/10.1590/1984-70332025v25n2a01>

Abstract: In the present study, a novel CYP86A22-like (CYP86A22L) was identified from *Citrus maxima* fruits. CmCYP86a22L contained most conserved motifs of plant CYP450 family, and its transcript levels was high in different fruit tissues but dramatically decreased during fruit development. To elucidate the specific role of the variable substrate recognition site (SRS) SRS6 region in CmCYP86A22L, C-terminal fragment containing SRS6 region was transiently expressed in tobacco leaves, and exogenous CmCYP86A22L mRNAs were significantly upregulated as expected. Furthermore, the stem diameters of CmCYP86A22L transient expression lines were wider than mock in 3~12 days after infiltration, accompanied by increases cell layers of xylem, phloem and cortex, and cortex cell volume. Additionally, the CmCYP86A22L transient expression stems lacked visible cuticle on epidermal cells. These results collectively suggested that CmCYP86A22L was involved in fruit development, and the SRS6 region of CmCYP86a22L could regulate stem growth.

Keywords: CYP86A22L, *Citrus maxima*, fruit development, stem growth, SRS6 region

INTRODUCTION

Cytochrome P450 (CYP450) monooxygenases are heme-containing enzymes that catalyze and synthesize a diverse range of metabolites in response to intrinsic growth, development, and biotic and abiotic stresses across plant, animal, and microorganism kingdoms (Pinot and Beisson 2011, Chakraborty et al. 2023). Recently, over 13,000 CYP450s in animals and more than 35,000 CYP450s in plants have been identified, annotated or named (Nelson and Werck-Reichhart 2011, Nelson 2018, Chakraborty et al. 2023). Representing the most diversified gene family, CYP450s constitute approximately 1% of encoding proteins in plants, mainly catalyze hydroxylation reactions, and contribute to the synthesis of biopolymer subunits such as lignin, cutin, suberin, sporopollenin, phytohormones, pigments, fragrances, flavors, antioxidants, and allelochemicals (Kumar et al. 2024).

Based on the amino acid sequence identity, the plant CYP450 superfamily has been clustered into 127 subfamilies, with terrestrial plants housing two main clans: single-family clans (CYP51, CYP74, CYP97, CYP710, CYP711, CYP727 and CYP746) and multifamily clans (CYP71, CYP72, CYP85 and CYP86) (Nelson and Werck-Reichhart 2011). As one of the most ancient subfamily



*Corresponding author:

E-mail: wcc@zjnu.cn

 ORCID: 0009-0007-3427-3495

Received: 01 November 2023

Accepted: 03 May 2024

Published: 28 March 2025

¹ Zhejiang Normal University, Wucheng District, Jinhua, Zhejiang, 321017, China

in terrestrial plants, the CYP86 clan primarily composes of fatty acid hydroxylases or alkane hydroxylases, essential for the production of vital biomolecules that cover the surfaces of aerial tissues, roots, and pollens (Nelson and Werck-Reichhart 2011). To date, eleven members of CYP86 subfamily in *Arabidopsis* have been characterized (<http://www-ibmp.u-strasbg.fr/~CYPedia/index.html#CYP86>). The first described CYP86 member was a fatty acid ω -hydroxylase based on consensus sequences from mammalian and yeast (Benveniste et al. 1998). AtCYP86A8, discovered from the mutant *lacerata*, plays important roles in regulating cell differentiation, apical dominance and senescence (Wellesen et al. 2001). Subsequently, the catalytic activities and biological functions of CYP86 members have been elucidated across different model plant species. Specifically, various CYP86 members have been characterized as fatty acid hydroxylases and oxidases involved in the biosynthesis of cutins, suberins and estolides, as well as in biotic and abiotic stress responses and reproduction processes (Benveniste et al. 1998, Pinot and Beisson 2011, Kumar et al. 2024). However, little research has been focused on functions of CYP86 members in horticultural crops, especially in pomelo.

In recent years, a spontaneous bud mutant of 'guanxi pomelo' (*Citrus maxima*), 'red-fleshed pomelo', had been identified to accumulate high concentrations of lycopene and β -carotene in the juice sac of fruit, with its fruit ripening period being approximately 20 days earlier (Liu et al. 2016). Based on our previous microarray-based expression analysis (unpublished data), the transcript levels of a *CYP86A22* like gene in 'red-fleshed pomelo' fruits displayed a significant difference compared to 'guanxi pomelo', suggesting that *CmCYP86A22L* might be involved in the process of fruit development. This present study aimed to investigate the potential roles of *CmCYP86A22L* during vegetative growth and fruit development. For this purpose, 'red-fleshed pomelo' and its corresponding wild-type 'guanxi pomelo' were used, and the coding sequence and expression patterns of *CmCYP86A22L* were investigated. In addition, the C-terminal *CmCYP86A22L* sequence containing relatively variable SRS6 region was transiently expressed in young leaves of *Nicotiana benthamiana*, and its effects on stem growth were also investigated.

MATERIAL AND METHODS

Plant materials

Six-year-old 'red-fleshed pomelo' and 'guanxi pomelo' (*Citrus maxima*) grown in the natural field of Quzhou Institute of Agricultural Sciences (lat 118° 93' E and long 28° 98' N, Quzhou, Zhejiang Province, China) were used in this study. The fruits were collected at 75, 105, 135, 165 and 195 days post anthesis (DPA) in 2019 and 2021, respectively. Following collection, the juice sac was separated from flavedo, albedo and segment membrane using the standard proposed by Liu et al. (2007), and then immediately frozen with liquid nitrogen, and stored at -80 °C until further analysis.

Tobacco (*Nicotiana benthamiana*) seedlings were cultured in plant growth chambers under controlled conditions of 22~23 °C, 16 h light/8 h dark photoperiod, and 80% relative humidity. Four-week-old young expanded leaves were used for agroinfiltration-based transient expression analysis.

Isolation and bioinformatic analysis of *CmCYP86A22L* gene

Total RNA extraction from pomelo juice sacs and transient expression stems, and 1st-strand cDNA synthesis were performed according to Liu et al. (2016). The open reading frame of *CmCYP86A22L* was amplified using specific primer pairs (Table S1) and Phusion High-Fidelity DNA Polymerase (New England Biolabs Inc., Beijing, China). Subsequently, sequence analyses were carried out according to Liu et al. (2016). A phylogenetic tree was constructed with MEGA 7.0 software using the neighbor-joining method and a 1000-replication bootstrap test, and the phylogenetic tree was visualized with online Evolview v3 software (<https://www.evolgenius.info/evolview/>).

Relative expression analysis of *CmCYP86A22L* during pomelo fruit development and homologous *NbCYP86A22L* in transient expression tobacco lines

Based on the known cDNA sequences, specific primers (Table S1 and Figure S1) of *CmCYP86A22L* and *NbCYP86A22L* (*CmCYP86A22L* homologous gene in tobacco) were designed for real-time quantitative polymerase chain reaction (qPCR) analysis. The qPCR system, procedures and data analysis were performed as previous described by Liu et al. (2016). The relative expression levels of *CmCYP86A22L* and *NbCYP86A22L* genes were normalized to reference genes *Cg β -tubulin* (Wang et al. 2013) and *NbEF1 α* (Ishihama et al. 2011), respectively.

Transiently expressing the variable SRS6 fragment of CmCYP86a22L in tobacco seedlings

Tobacco rattle virus (TRV)-induced gene silencing vectors pTRV1, pTRV2, pTRV2-GFP and pTRV2-NbPDS (conserved *phytoene desaturase* fragment) were kindly provided by Professor Xinzhong Cai (Zhejiang University, Hangzhou, China). The C-terminal fragment (from 1,363 to 1,562, 200 bp) containing the variable SRS6 region of *CmCYP86A22L* was inserted into the pTRV2 vector. Then, vectors pTRV1, pTRV2-GFP, pTRV2-NbPDS, and the reconstructed pTRV2-CmCYP86A22L were transformed into *Agrobacterium tumefaciens* GV3101, respectively.

For transient expression in tobacco leaves, *Agrobacterium* carrying pTRV2-CmCYP86A22L and pTRV1 at a 1:1 ratio were coinfiltrated (Liu et al. 2002), along with negative control pTRV2-GFP (mock) and positive control pTRV2-NbPDS. The experiments were performed at least three times, and young expanded leaves from 20 individual lines were used.

The basal stems (0.5 cm above stem base) from mock and *CmCYP86A22L* transient expression lines were harvested at 0 d and 10 d after agroinfiltration for morphological and anatomical observation. Specific stages of stem samples were collected and then stored at -80 °C until used for relative gene expression analysis.

Stem paraffin section preparation and microscopy observation for *CmCYP86A22L* transient expression stems

Five tobacco basal stems from *CmCYP86A22L* transient expression lines and mock at 0 d and 10 d after agroinfiltration were randomly collected, immediately fixed in formaldehyde-acetic acid-ethanol solution (37% formaldehyde, 5% glacial acetic acid and 50% ethanol), and vacuumed for more than 24 h. The stems were then processed for dehydration, clearing, embedding, transverse slicing, rehydration and staining as described previously (Chen et al. 2015). The transection slides were scanned with Virtual Slide Microscopy VS120 (Olympus Co., Ltd, Shanghai, China).

Statistical analysis

The data collected in this study were analyzed using the SPSS 20.0 software and expressed as mean values with standard deviations ($n \geq 3$). Statistical significance was determined using one-way analysis of variance (ANOVA) with independent-samples t test. P values of less than 0.05 were considered to be statistically significant.

RESULTS AND DISCUSSION

Sequence and structure analysis of *CmCYP86A22L*

The full-length *CYP86A22L* cDNAs (NCBI accession number: KM259904), isolated from juice sacs of 'red-fleshed pomelo' and 'guanxi pomelo' immature fruits, were completely identical, containing an open reading frame of 1,626 bp, and encoding 541 amino acid residues with a calculated molecular mass of 61.39 kDa and a predicted isoelectric point of 7.83. The C-terminal region of *CmCYP86A22L* harbored a conserved heme binding motif (FxxGxRxCxG, Figures S2), which is recognized as CYP450 catalytic center with heme ions binding to the thiolate of a conserved cysteine (Bak et al. 2011). In addition, several highly conserved motifs, characteristics of the CYP86 subfamily, were also identified within *CmCYP86A22L*, including a proline-rich segment in the N-terminus for membrane hinge, a PERF/W motif for plant CYP450 clade signature, an I-helix motif (AGxDT) for oxygen binding and activation, and an ERR triad for locking heme pockets (Figure S2, Bak et al. 2011).

Substrate recognition site (SRS) regions were predicted to define CYP450 catalytic specificity and variability relative to substrates and metabolites (Duan and Schuler 2005, Lui et al. 2020, Toporkova et al. 2020). Compared to homologous sequences from different plant species, the putative SRS regions of *CmCYP86A22L* were highly conserved in the SRS1 and SRS4 regions, relatively variable in the SRS5 region, distinctly variable in the SRS2 and SRS6 regions, and absent in the SRS3 region (Figures 1 and S2).

Phylogenetic analysis revealed that *CmCYP86A22L* was orthologous to *C. maxima* Cg5g002560, *C. sinensis* Cs5g03440 and *CsCYP86A22L* protein XP_006476545, and demonstrated significant conservation with CYP86A22L sequences from *Hibiscus syriacus*, *Mangifera indica*, *Juglans regia*, and others (Figure 1). In addition, *CmCYP86A22L* shared high identities with *A. thaliana* CYP86A8 (AT2G45970, 72.69%) and CYP86A7 (AT1G63710, 71.86%). *AtCYP86A7* and *AtCYP86A8* have been reported to catalyze the ω -hydroxylation of saturated and unsaturated C12 to C18 fatty acids, as well as auric acids

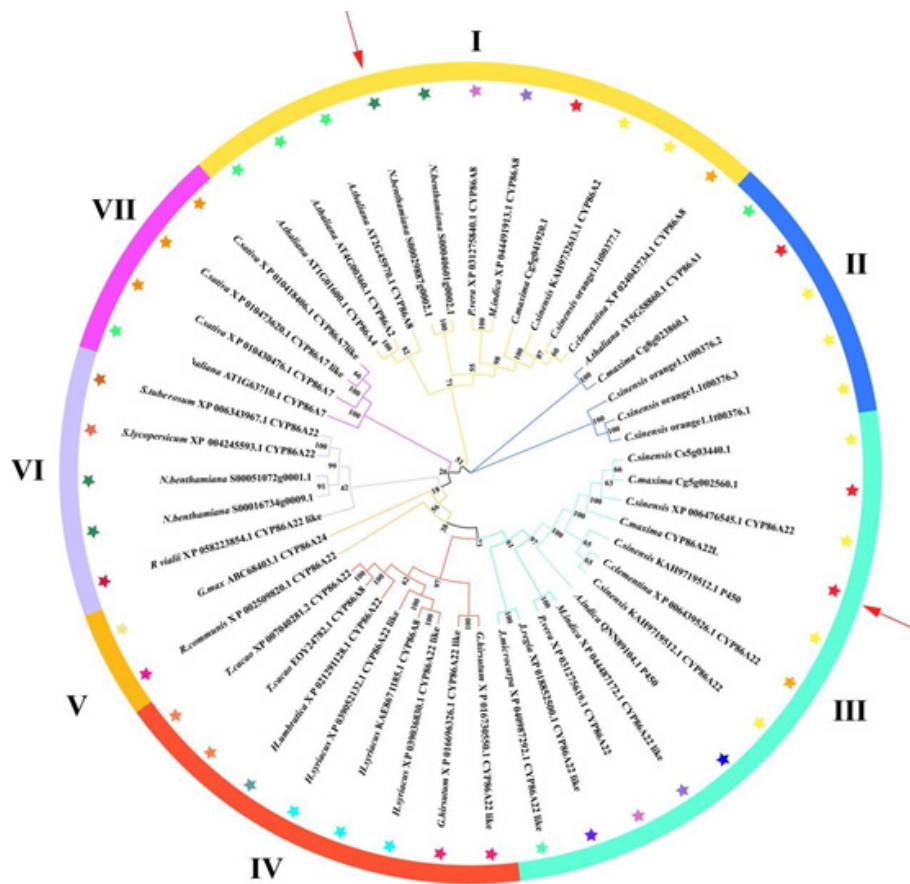


Figure 1. Phylogenetic tree of CmCYP86A22L and other plant CYP86A members. Arrows indicated the locations of CmCYP86A22L, and CmCYP86A22L homolog NbCYP86a22L.

to ω -hydroxylauric acids (Duan and Schuler 2005). Moreover, AtCYP86A8 displayed higher efficiency in metabolizing saturated medium-chain fatty acids and unsaturated oleic acids compared with saturated short-chain lauric acids (Rupasinghe et al. 2007). These findings supported the hypothesis that CmCYP86A22L is a fatty acid ω -hydroxylase, and the distinct sequence variation of CYP86As across different plant species indicated their unique biological functions throughout evolution.

Expression patterns of CmCYP86A22L gene during ‘red-fleshed pomelo’ and ‘guanxi pomelo’ fruit development

Espelie et al. (1980) reported that the juice sac of ripening grapefruit (*C. paradisi*) contained a thin layer of cuticle and significantly reduced polymer and wax contents in comparison to leaf, fruit peel and seed coat, implying that less CYP86A was synthesized in the juice sacs of citrus fruits. Similarly, the relative expression levels of CmCYP86A22L in the juice sacs of ‘red-fleshed pomelo’ and ‘guanxi pomelo’ fruits significantly decreased during fruit development and ripening, with CmCYP86A22L mRNAs in young fruits (DAF75) of both cultivars being approximately 100-fold higher than those in ripening fruits (DAF195). Moreover, CmCYP86A22L transcripts in young fruits of ‘red-fleshed pomelo’ were 7.7-fold higher than those in developing fruits at DAF105, while CmCYP86A22L transcripts of ‘guanxi pomelo’ juice sacs notably decreased from DAF105 (Figure 2a). Compared to ‘guanxi pomelo’, greater reduction in CmCYP86A22L transcripts in ‘red-fleshed pomelo’ juice sacs, suggesting a lower accumulation of cuticle.

Given the complete homology between CmCYP86A22L and Cg5g002560 cDNA sequences, the expression pattern of CmCYP86A22L gene was further analyzed in different tissues and fruit developmental stages using ‘Wanbaiyou’ pomelo

transcriptomic data (<http://citrus.hzau.edu.cn/geneExpression/query.php>). As shown in Figure 2b, *CmCYP86A22L* gene expression was lower in root tip, leaf, petal primordium and stamen primordium (PPSP), but higher levels in fruit tissues like flavedo, albedo, segment membrane (SM) and juice sac (JS). Interestingly, *CmCYP86A22L* exhibited the highest expression levels in the young fruit (DAF80), followed by a sharp decline in the developing fruit (DAF140). This trend was also observed for the *AtCYP86A8* gene, which was strongly expressed in growing seedling, inflorescence and silique, and has pleiotropic functions in regulating cell differentiation in epidermis, apical dominance, senescence and leaf shape (Wellesen et al. 2001). Moreover, expression levels of *S. lycopersicum* *SICYP86A69* gene, which contributed to cutin monomer production on the fruit surface, were also significantly downregulated during fruit development and ripening with a higher expression level in the exocarp than the mesocarp (Shi et al. 2013). These observations led to the hypothesis that *CmCYP86A22L* may involve in cuticle and wax synthesis during early fruit development.

Transient expression of *CmCYP86A22L* fragment containing SRS6 region promoted tobacco stem thickening

As described above, the SRS6 region of *CmCYP86A22L* was distinctly variable in different plant species. To explore its specific function, a 200-bp fragment of *CmCYP86A22L* containing the SRS6 segment was transiently expressed in tobacco leaves mediated by the TRV system. Seven days after agroinfiltration, the young upper leaves of tobacco began to exhibit a photo-bleached phenotype caused by the absence of *NbPDS* gene (Figure S4), which was easily evaluated for agroinfiltration efficiency (Liu et al. 2002). However, no phenotype change was observed in the new-growth and infiltrated leaves of mock and *CmCYP86A22L* transient expression lines (Figure S3), while stems of *CmCYP86A22L* transient expression lines became thicker than those of mock plants from the 3~5th day post agroinfiltration (DPA, Figure 3a), and this difference reached the highest at 13th DPA.

Due to the lack of visible change in stem thickness, the anatomical structures of mock and *CmCYP86A22L* transient expression stems were analyzed. As shown in Figures 4a and 4c, no obvious difference was observed between the mock and the *CmCYP86A22L* transient expression stems at 0 DPA. However, the *CmCYP86A22L* transient expression stems at 10 DPA exhibited visibly absent cuticle on epidermal cells, indicating that the epidermal cells or cell walls in these *CmCYP86A22L* transient expression stems were easily destroyed. Furthermore, *CmCYP86A22L* transient expression stems produced more xylem and phloem cells in stems (Table 1), and a noticeable increase

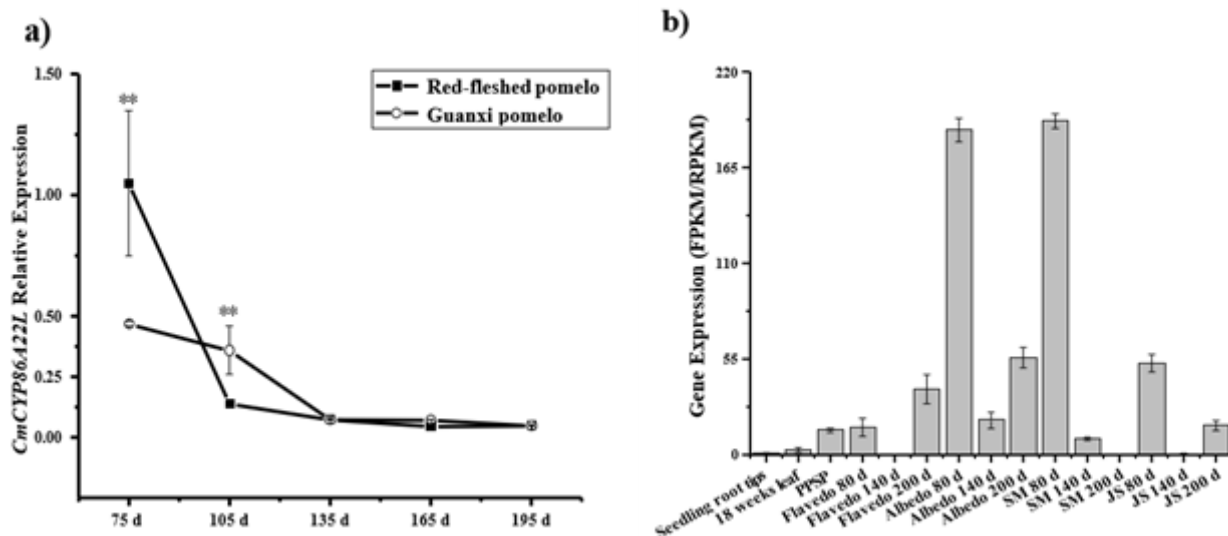


Figure 2. *CmCYP86A22L* gene expression profiles. **a)** *CmCYP86A22L* relative expression levels in the juice sac of ‘red-fleshed pomelo’ and ‘Guanxi pomelo’ during fruit development. **b)** *CYP86A22L* expression patterns in different ‘Wanbaiyou’ pomelo tissues and fruit developmental stages from transcriptomic data (<http://citrus.hzau.edu.cn/geneExpression/query.php>). JS referred to juice sacs; PPSP referred to petal primordia and stamen primordia; SM referred to segment membrane; d referred to days after flowering. Error bars represent the standard deviation of three biological replicates. **represented $p < 0.01$.

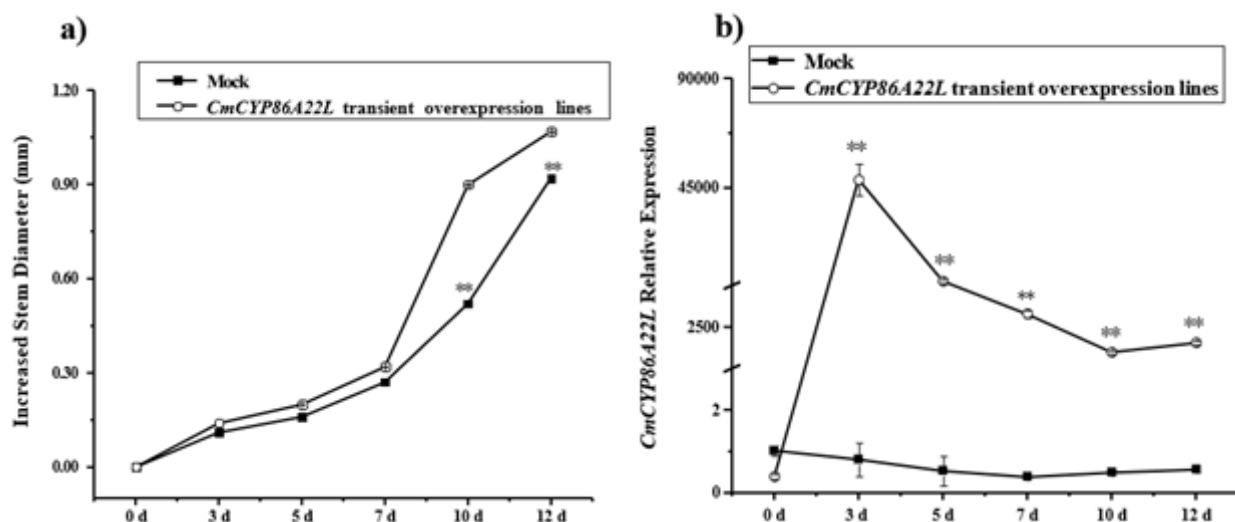


Figure 3. Transient expressed CmCYP86A22L increased stem diameter. **a)** Relative expression levels of CmCYP86A22L. **b)** Increased stem diameter. Mock referred to the negative control with Agrobacteria carrying pTRV -GFP and pTRV at a 1:1 ratio. ** represented $p < 0.01$, and * represented $0.01 < p < 0.05$.

Table 1. Increased cell layers in the stems of CmCYP86A22L transient expression lines and mocks

	xylem	phloem	cortex
Mock	11.37 ± 0.89	4.06 ± 0.53	3.31 ± 0.53
CmCYP86A22L transient expression lines	13.85 ± 0.99**	5.52 ± 0.88**	4.07 ± 0.79*

Mocks were the negative lines coinfiltrated with Agrobacteria carrying pTRV2-GFP and pTRV1 at a 1:1 ratio. ** represented $p < 0.01$, and * represented $0.01 < p < 0.05$.

in cortex cell volume when compared to mock (Figure 4). Wellesen et al. (2001) had previously identified that *Arabidopsis* CYP86A8 could alter cell differentiation in the leaf epidermis, delay senescence, and reduce apical dominance through lipid metabolism regulation. Based on these findings, it appeared that CmCYP86A22L is a fatty acid ω -hydroxylase to regulate stem development, especially through the proliferation of xylem and phloem cells and the expansion of cortex cell.

TRV systems have been successfully developed for biotechnology and basic science application through virus-induced gene silencing, foreign polypeptide expression, and CRISPR/Cas9-based genome editing (Liu et al. 2002, Wang et al. 2020). Theoretically, DNA fragments with a minimum of 23 continuous nucleotides bearing 100% identity to endogenous targeted genes are necessary for gene silencing (Burch-Smith et al. 2004). In this study, only 17 continuous specific nucleotides of CmCYP86A22L C-terminal sequence were 100% identical to the endogenous target *NbCYP86A22L*, which seemed to promote exogenous gene expression rather than gene silencing. Moreover, the exogenous CmCYP86A22L mRNAs were low or could not be detected in the transient expression stems at 0 DPA and in the mock stems from 0 to 12 DPA, while CmCYP86A22L mRNAs rapidly accumulated, and gradually decreased in the CmCYP86A22L transient expression stems from the 3rd DPA (Figure 3b). In addition, the relative expression levels of endogenous *NbCYP86A22L* gene (CmCYP86A22L homogenous gene, Niben101Scf02264g06012) in stems of CmCYP86A22L transient expression lines were significantly higher than those of mock from 3 DPA (Figure S4), which meant tobacco rattle virus affected endogenous *NbCYP86a22L* transcription, and transient expressing CmCYP86A22L recovered partially *NbCYP86a22L* transcription. Xiao et al. (2004) reported that *AtCYP86A2* expression could be repressed by infecting with compatible, incompatible, or nonhost *Pseudomonas syringae* strains. Similarly, *NbCYP86A22L* mRNAs in the CmCYP86A22L transient expression stems were somewhat higher than those of the mock, indicating that CmCYP86A22L was also probably involved in plant defense responses.

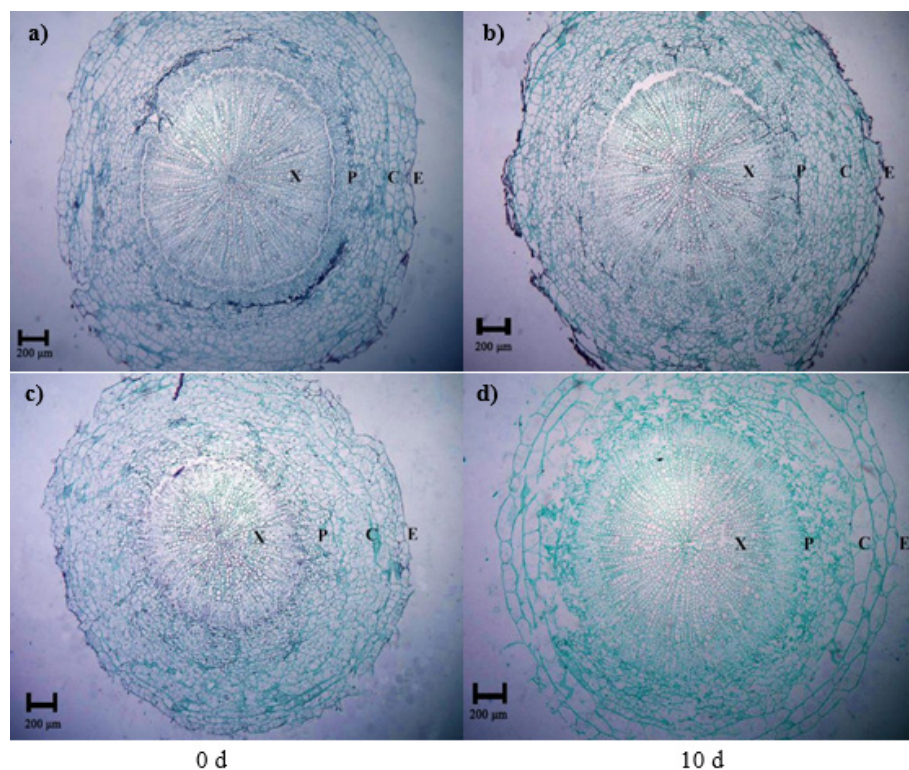


Figure 4. Transverse section of mock (a and b) and *CmCYP86A22L* transient expression stems (c and d) after coinfiltration at 0 and 10 day. E referred to epidermis, C referred to cortex, P referred to phloem, and X referred to xylem.

CONCLUSIONS

In this study, *CYP86A22L* cDNA sequences isolated from ‘red-fleshed pomelo’ and ‘guanxi pomelo’ were completely identical and showed extremely high homologous with *Citrus* species and *A. thaliana* CYP86A8 and CYP86A7, suggesting that *CmCYP86A22L* evolved conservatively in citrus species and terrestrial plants. The expression levels of *CmCYP86A22L* were high in tissues of flavedo, albedo, segment membrane and juice sac, but significantly decreased during fruit development. After transiently expressed the C-terminal *CmCYP86A22L* fragment containing the variable SRS6 region in young tobacco leaves, the exogenous *CmCYP86A22L* mRNAs accumulated rapidly and significantly in the basal tobacco stems. Additionally, the basal stem diameters of the *CmCYP86A22L* transient expression lines were observed to be wider than those of the mock in 3~12 days, following periclinal division of xylem and phloem, along with cortex cell expansion. Taken these results together, *CmCYP86A22L* was act as a fatty acid ω -hydroxylase and participated in stem and fruit development. These findings provided new insights into CYP86A22L functional characterization, laying a foundation for developing molecular breeding programs aimed on the regulation of vegetative and reproductive organ development

ACKNOWLEDGMENTS

This work was supported by the Natural Science Foundation of Zhejiang Province (LY20C140002).

DATA AVAILABILITY

The datasets generated and/or analyzed in this study, as well as the supplementary tables and figures, are available from the corresponding author upon reasonable request.

REFERENCES

- Bak S, Beisson F, Bishop G, Hamberger B, Höfer R, Paquette S and Werck-Reichhart D (2011) Cytochromes P450. **The Arabidopsis Book 9**: e0144.
- Benveniste I, Tijet N, Adas F, Philipps G, Salaün JP and Durst F (1998) CYP86A1 from *Arabidopsis thaliana* encodes a cytochrome P450-dependent fatty acid omega-hydroxylase. **Biochemical and Biophysical Research Communications 243**: 688-693.
- Burch-Smith TM, Anderson JC, Martin GB and Dinesh-Kumar SP (2004) Applications and advantages of virus-induced gene silencing for gene function studies in plants. **The Plant Journal 39**: 734-746.
- Chakraborty P, Biswas A, Dey S, Bhattacharjee T and Chakrabarty S (2023) Cytochrome P450 gene families: role in plant secondary metabolites production and plant defense. **Journal of Xenobiotics 13**: 402-423.
- Chen BY, Wang CH, Tian YK, Chu QG and Hu CH (2015) Anatomical characteristics of young stem and mature leaves of dwarf pear. **Scientia Horticulturae 186**: 172-179.
- Duan H and Schuler MA (2005) Differential expression and evolution of the Arabidopsis CYP86A subfamily. **Plant Physiology 137**: 1067-1081.
- Espelie KE, Davis RW and Kolattukudy PE (1980) Composition, ultrastructure and function of the cutin- and suberin-containing layers in the leaf, fruit peel, juice-sac and inner seed coat of grapefruit (*Citrus paradisi* Macf.). **Planta 149**: 498-511.
- Ishihama N, Yamada R, Yoshioka M, Katou S and Yoshioka H (2011) Phosphorylation of the *Nicotiana benthamiana* WRKY8 transcription factor by MAPK functions in the defense response. **The Plant Cell 23**: 1153-1170.
- Kumar R, Radhamani J and Rajkumar S (2024) Exploration of allelic diversity reveals a novel FAD2 (Oleate desaturase) gene in *Brassica juncea*. **Crop Breeding and Applied Biotechnology 24**: e47702424
- Liu Q, Xu J, Liu YZ, Zhao XL, Deng XX, Guo LL and Gu JQ (2007) A novel bud mutation that confers abnormal patterns of lycopene accumulation in sweet orange fruit. **Journal of Experimental Botany 58**: 4161-4171.
- Liu WN, Ye Q, Jin XQ, Han FQ, Huang XZ, Cai SH and Yang L (2016) A spontaneous bud mutant that causes lycopene and β -carotene accumulation in the juice sacs of the parental Guanxi pummelo fruits (*Citrus grandis* (L.) Osbeck). **Scientia Horticulturae 198**: 379-384.
- Liu YL, Schiff M, Marathe R and Dinesh-Kumar SP (2002) Tobacco Rar1, EDS1 and NPR1/NIM1 like genes are required for N-mediated resistance to tobacco mosaic virus. **The Plant Journal 30**: 415-429.
- Lui ACW, Lam PY, Chan KH, Wang LX, Tobimatsu Y and Lo C (2020) Convergent recruitment of 5'-hydroxylase activities by CYP75B flavonoid β -ring hydroxylases for tricin biosynthesis in Medicago legumes. **New Phytologist 228**: 269-284.
- Nelson D and Werck-Reichhart D (2011) A P450-centric view of plant evolution. **The Plant Journal 66**: 194-211.
- Nelson DR (2018) Cytochrome P450 diversity in the tree of life. **Biochim Biophys Acta-Proteins Proteomics 1866**: 141-154.
- Pinot F and Beisson F (2011) Cytochrome P450 metabolizing fatty acids in plants: characterization and physiological roles. **FEBS Journal 278**: 195-205.
- Rupasinghe SG, Duan H and Schuler MA (2007) Molecular definitions of fatty acid hydroxylases in Arabidopsis thaliana. **Proteins 68**: 279-293.
- Shi JX, Adato A, Alkan N, He Y, Lashbrooke J, Matas AJ, Meir S, Malitsky S, Isaacson T, Prusky D, Leshkowitz D, Schreiber L, Granell AR, Widemann E, Grausem B, Pinot F, Rose JKC, Rogachev I, Rothan C and Aharoni A (2013) The tomato SISHINE3 transcription factor regulates fruit cuticle formation and epidermal patterning. **New Phytologist 197**: 468-480.
- Toporkova YY, Smirnova EO, Mukhtarova LS, Gorina SS and Grechkin AN (2020) Catalysis by allene oxide synthases (CYP74A and CYP74C): alterations by the Phe/Leu mutation at the SRS-1 region. **Phytochemistry 169**: 112-152.
- Wang LH, Pan YJ, Yang L, Cai SH and Huang XZ (2013) Validation of internal reference genes for qRT-PCR normalization in 'Guanxi Sweet Pummelo' (*Citrus grandis*). **International Journal of Fruit Science 30**: 48-54.
- Wang M, Gao SL, Zeng WZ, Yang YQ, Ma JF and Wang Y (2020) Plant virology delivers diverse toolsets for biotechnology. **Viruses 12**: 1338.
- Wellesen K, Durst F, Pinot F, Benveniste I, Nettekheim K, Wisman E, Steiner-Lange S, Saedler H and Yephremov A (2001) Functional analysis of the LACERATA gene of Arabidopsis provides evidence for different roles of fatty acid omega-hydroxylation in development. **Proceedings of the National Academy of Sciences of the United States of America 98**: 9694-9699.
- Xiao FM, Goodwin SM, Xiao YM, Sun ZY, Baker D, Tang XY, Jenks MA and Zhou JM (2004) Arabidopsis CYP86A2 represses *Pseudomonas syringae* type III genes and is required for cuticle development. **EMBO Journal 23**: 2903-2913.